Proceedings of the
Annual Stability Conference
Structural Stability Research Council
Louisville, Kentucky, April 1-4, 2025

Determination of minimum concrete layer in hollow concrete-filled steel tubular columns using plate buckling in an elastic medium

Mashudha Sulthana[1], Surya Prasanth M.[2]

Abstract

In long-column rectangular concrete-filled steel tubular cross-sections, concrete filling primarily prevents local instabilities and is less significant in improving global buckling. Further, the concrete contribution to flexural resistance is limited in CFST. Therefore, filling concrete only in the periphery is preferable, as in the case of a hollow concrete-filled steel tubular (H-CFST) cross-section. This paper finds the minimum concrete thickness sufficient to prevent local instabilities in the steel tube by solving plate buckling on an elastic medium problem. A closed-formed solution for a uniformly thick plate in contact with an elastic medium (here, a concrete layer of a minimum thickness) is obtained by assuming a sinusoidal deformation in both directions of the plate at the point of instability. The minimum concrete wall thickness required to prevent plate buckling in H-CFST is proposed as a function of the width-to-thickness of the steel plate, steel yield strength and the grade of concrete. The proposed value is validated with the test results on H-CFST columns from the literature. An extensive database on H-CFST is developed numerically using finite element (FE) software to compensate for the limited test data available on H-CFST columns. The parameters considered for the database are the width-to-thickness ratio of the steel tube, the grade of steel, the grade of concrete, and the length-of-width ratio of the column. The minimum concrete thickness proposed in this study is used in developing the FE model, and delayed elastic plate buckling is observed from the results, similar to a CFST column. The ultimate capacity of the specimens from the FE results is compared with the AISC-360 specifications for compact CFST cross-sections. They are in good agreement, with a mean and standard deviation of 1.03 and 0.07. The present findings help in the design optimization of CFST columns, ensuring stability and economy.

1. Introduction

The Hollow Concrete-filled Steel Tubular (H-CFST) cross-section (Fig. 1) is an innovative variation of Concrete-filled Steel Tube (CFST), where a vacant space is left at the core and concrete is filled at the periphery. CFST is used in buildings and bridges for their superior structural performance and fast-track construction (Han et al. 2014). It is popular for its enhanced

[1] Assistant Professor, Department of Civil Engineering, National Institute of Technology Tiruchirappalli, India <smash@nitt.edu>
[2] Doctoral Research Scholar, Department of Civil Engineering, National Institute of Technology Tiruchirappalli, India <surya.prasanth111@gmail.com>

axial compressive strength due to concrete confinement and delay in the local buckling of steel. However, in a practical scenario where the dimensionless slenderness of the column is greater than 0.5, concrete confinement is not found (EN 1994-1-1 2004). Further, the concrete infill is helpful in preventing and delaying local instabilities rather than preventing the global buckling of the column. Therefore, it is more beneficial to fill the steel tube with concrete only in the periphery, as in the case of H-CFST. Concrete-filled double steel tubular (CFDST) is a type of CFST with a vacant inner core similar to H-CFST but with a steel tube lining the inner surface of the concrete. In CFDST, the inner steel tube does not contribute to the concrete confinement effect (Han et al. 2004; Tao et al. 2004; Zhao and Grzebieta 2002). Further, in the case of long columns, the inner steel contributes less to the member buckling resistance (Essopjee and Dundu 2015; Romero et al. 2015). Therefore, providing the inner steel tube is not really useful, and H-CFST is a preferable cross-section.

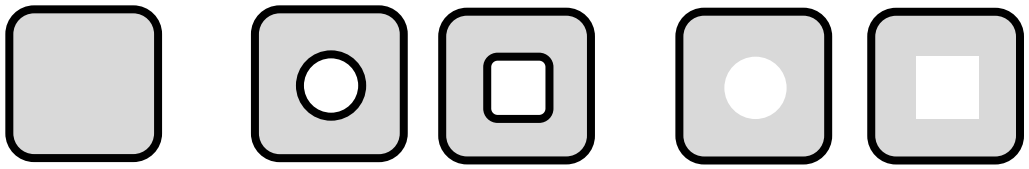

(a) CFST (b) CFDST (c) H-CFST

Figure 1: Variants in square concrete-filled steel tubular cross-sections

H-CFST has a higher strength-to-weight ratio. The hollow nature of HCFT columns allows for better drainage and reduced moisture accumulation, which mitigates the risk of internal corrosion and enhances the durability of the structure (Kuranovas and Kvedaras 2007a). The reduced mass of HCFT columns can lead to improved seismic behavior, as lighter structures experience lower seismic forces, contributing to a more resilient building during an earthquake. By reducing the amount of concrete required, HCFT columns optimize material usage, leading to potential cost savings in both material and construction time. H-CFST is manufactured by the centrifugal method of concrete filling. In a study by Kuranovas and Kvedaras (2007b), the spinning velocity and concrete mix proportioning suitable for centrifugation of the H-CFST specimen have been discussed. Concreting in H-CFST could also be achieved by placing a permanent formwork made of thin corrugated sheet (Prasanth and Sulthana 2024a), or a polyvinyl chloride pipe or a filler material (Prasanth and Sulthana 2024b).

Satoshi et al. (1996a) tested 26 circular H-CFST specimens and 26 square H-CFST specimens developed using centrifugal concreting technique. The width-to-thickness ratio of the steel tube, steel yield strength, concrete grade and hollowness ratio are the parameters considered for the experimental evaluation. Out of the total 52 specimens, 20 specimens have been loaded on the concrete surface alone. The capacity is increased by 100% by loading on the concrete surface alone in the case of circular H-CFST and 50% in the case of square H-CFST. On loading the specimens uniformly on the steel and concrete surfaces, the test results show an increase in the strength of around 20% in the case of circular H-CFST and 5-10% in the case of square H-CFST. Even though the ultimate capacity of the specimens under concrete-alone loaded conditions is higher, the stiffness is lower than those specimens loaded uniformly on the steel and concrete surfaces. This phenomenon is similar to CFST specimens (Johansson and Gylltoft 2002). The increase in the hollowness ratio from 5% to 50% decreases the confining effect from 10% to 5% in the case of a

square tube and 20% to 14 % in the case of a circular tube. It should be noted that the decrease in weight is much higher than the strength decrement, which accounts for the improved strength-to-weight ratio of an H-CFST column. An increase in the width-to-thickness ratio and the concrete grade reduces the confining effect similar to a CFST cross-section. Based on the test results, Satoshi et al. (1996b) have proposed an analytical expression to evaluate the confining effect in the H-CFST cross-sections. Satoshi et al. (1997) tested 12 circular and 12 square H-CFST under cyclic flexure. The ultimate bending moment of the specimens is higher than the analytical predictions for all hollowness ratios ranging from 5% to 50%. Width-to-thickness ratio, steel yield strength and concrete grade are the other parameters considered for the experimental studies. The hysteretic curve shows that the energy dissipation is lesser for increasing hollowness ratios in the H-CFST specimens. Kuranovas and Kvedaras (2007a) have tested the axial compressive behavior of six circular H-CFSTs of diameter-to-thickness ratio 44, prepared through single and double-layer centrifugation of concrete layer thickness around 16 mm. The compressive capacity of the test specimens matches the AISC-360 capacity equations. Zhao et al. (2019) studied the axial compressive behavior of circular H-CFST analytically and numerically, and they proposed an expression for accurate predictions of the axial compressive capacity to account for the concrete confinement effect. Sulthana and Jayachandran (2017) have reported the long column behavior of H-CFST square columns and compared them with the CFDST columns. It was found that the contribution of the inner steel tube in CFDST is lesser for long columns, and an H-CFST is more effective in load resistance than CFDST and CFST in long columns.

Even though there are a few studies found in the literature on the axial load behavior of square H-CFST columns, the need to find the optimum thickness of the concrete layer in H-CFST has not been addressed yet. The present study focuses on determining the minimum concrete thickness that is needed to prevent local buckling. The plate element with the concrete layer in the H-CFST is assumed to be a plate on an elastic medium, and the plate buckling stress is found by solving the plate equations. A semi-empirical expression is proposed to find the minimum concrete thickness, and it is validated with the available test results. Finite element (FE) models are developed using ABAQUS software to compensate for the scarcity of H-CFST specimen data in the available literature data. The validated mode is further used for parametric studies. The width-to-thickness ratio of the steel tube, steel yield strength, concrete grade, and length-to-width ratio are the parameters considered when evaluating the proposed expression numerically. The FE results are compared with the ANSI/AISC 2016 specifications for a compact CFST under axial compression. The FE results are in good agreement with the code predictions that show the validity of the proposed expression.

2. Plate buckling on an elastic medium

Under axial compression, a slender plate element in a steel tube will undergo local buckling and the width-to-thickness limitations are prescribed in the design standards to define a slender plate element. However, this limit is relaxed in a concrete-filled steel tube (CFST) as the concrete filling delays and prevents the steel plate buckling. Similar to the CFST column, in the Hollow concrete-filled steel tubular (H-CFST) column, the local steel tube buckling will be delayed due to the presence of concrete. Fig. 1a shows an H-CFST column subjected to axial compression. Here, the objective is to find the minimum thickness of concrete that can prevent local buckling. The concrete layer is modelled as multiple linear springs linearly distributed over the surface of the steel plate. A plate element in the H-CFST column with a concrete layer as linear springs is

depicted in Fig. 1b. The plate edges with no loads are assumed to be simply supported. The width of the plate on the loaded, and no-load edges are *a* and *b*, respectively. Under axial compression, the plate may undergo buckling and the probable deformed shape is shown in Fig. 1c.

2.1 Plate buckling equation

The governing differential equation for a simply supported plate element on an elastic surface (due to the presence of a concrete layer) and subjected to a uniformly distributed axial compressive load is in Eq. 1, where k is the spring stiffness of the concrete layer of thickness t_c, D_s is the flexural rigidity of the steel plate element, N_x is the axial compressive load, and w is the transverse deflection in the plate due to buckling. A sinusoidal function is assumed as the deformed shape of the buckled plate (Eq. 2), where m and n are the numbers of half-sine waves in the y and x directions, respectively. Substituting Eq. 2 in Eq. 1 and solving for N_x, we get Eq. 3.

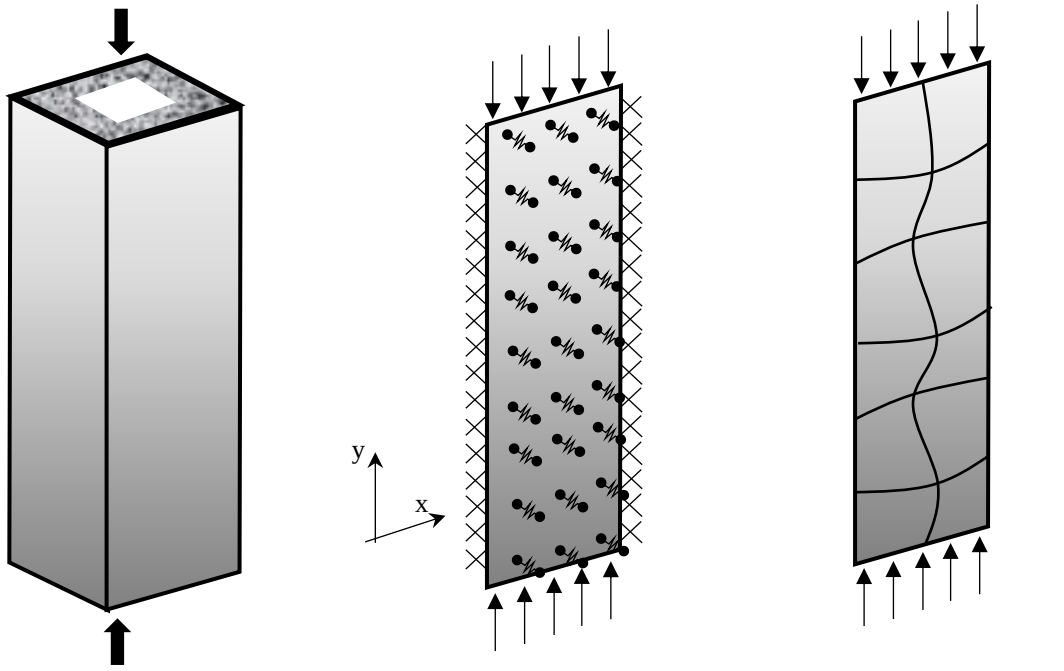

(a) Square H-CFST

(b) A H-CFST plate element with spring supports simulating the concrete layer

(c) Buckled H-CFST plate element

Figure 2: Hollow concrete-filled steel tube (H-CFST) under axial compression

$$D_s \nabla^4 w + N_x \frac{\partial^2 w}{\partial x^2} + kw(x,y) = 0 \tag{1}$$

$$w = \sum_{m=1}^{\infty}\sum_{n=1}^{\infty} A_{mn} \sin\frac{m\pi x}{a} \sin\frac{n\pi y}{b} \tag{2}$$

$$N_x = \left\{ \frac{k}{D_s \pi^2} + \pi^2 \left[\frac{m^2}{a^2} + \frac{n^2}{b^2} \right]^2 \right\} \frac{D_s a^2}{m^2} \tag{3}$$

At the critical buckling load, the number of half-sine waves in the x direction will be the least. Therefore, n is assumed as unity (Eq. 4). Further, at the stationary point, Eq. 4 is differentiated with respect to m to find the number of half waves formed at the point of instability (i.e., at the critical buckling load).

$$N_x = \left\{ \frac{k}{D_s \pi^2} + \pi^2 \left[\frac{m^2}{a^2} + \frac{1}{b^2} \right]^2 \right\} \frac{D_s a^2}{m^2} \tag{4}$$

$$\frac{dN_x}{dm} = 0 \Rightarrow m = \left[\frac{1.5ka^4}{\pi^4 D_s} + \frac{a^4}{b^4} \right]^{\frac{1}{4}} \tag{5}$$

2.2 Concrete stiffness

To find the spring stiffness of the concrete layer, the surface of the concrete in contact with the steel plate is assumed to have deformed in the same pattern as the steel plate to ensure compatibility. At the point of buckling, the concrete layer could be considered as a simply supported plate subjected to uniformly distributed transverse loading. The deflection formula for this type of plate is given in Eq. 6, where q_o is the uniformly distributed transverse load on the plate, and D_c is the flexural rigidity of the concrete layer (or plate). If the length of plate a is much larger than the width b, say $a > 10b$, Eq. 6 can be reduced to Eq. 7.

$$w = \frac{q_o}{\pi^4 D_c \left[\frac{1}{a^2} + \frac{1}{b^2} \right]^2} \tag{6}$$

$$w = \frac{q_o b^4}{\pi^4 D_c} \tag{7}$$

The concrete spring stiffness k is found in Eq. 8. Now, substituting Eq. 8 in Eq. 5, the number of half sine waves along the length of the plate at critical buckling load is in Eq. 9. We can understand that if there is no concrete layer, the m value is a/b, which is same as the solution from the conventional plate buckling problem. (Timoshenko et al. 1962).

$$k = \frac{q_o}{w} = \frac{\pi^4 D_c}{b^4} \tag{8}$$

$$m = \frac{a}{b} \left[\frac{1.5D_c}{D_s} + 1 \right]^{\frac{1}{4}} \tag{9}$$

2.3 Critical buckling stress

To find the critical plate buckling stress, Eq. 9 is substituted in Eq. 4. The final expression for the critical buckling stress of a plate on an elastic medium (here, a concrete layer) is given in Eq. 10. Here, the flexural rigidity of concrete and steel plate, D_c and D_s, respectively are expressed in Eq. 11 and Eq. 12. Eq. 10 is in a similar form to the critical buckling of a plate (Eq. 13), where K represents the square bracketed term in Eq. 10. Also, if there is no concrete, i.e., when $D_c = 0$, $K = 4$, which is the buckling factor in the case of a simply supported plate subjected to uniform axial compression.

$$\sigma_x = \frac{\pi^2 E_s}{12\left(1-\nu^2\right)\left(\frac{b}{t_s}\right)^2}\left[\frac{\frac{D_c}{D_s}}{\left(\frac{1.5D_c}{D_s}+1\right)^{1/4}}+\left\{\left(\frac{1.5D_c}{D_s}+1\right)^{1/4}+\frac{1}{\left(\frac{1.5D_c}{D_s}+1\right)^{1/4}}\right\}\right] \tag{10}$$

$$D_c = \frac{E_c t_c^3}{12\left(1-\nu_c^2\right)} \tag{11}$$

$$D_s = \frac{E_s t_s^3}{12\left(1-\nu_s^2\right)} \tag{12}$$

$$\sigma_x = \frac{K\ \pi^2 E}{12\left(1-\nu^2\right)\left(\frac{b}{t_s}\right)^2} \tag{13}$$

3. Finding the minimum concrete thickness

The minimum thickness of the concrete layer to prevent plate buckling for a given width-to-thickness ratio of the steel tube (b/t_s), steel yield strength (f_y) and concrete grade (f_c') has to be found using Eq. 10. However, the solution will not be simple that could be used for design. Therefore, graphs are plotted so that a semi-empirical solution can be proposed by regression analysis. For a conventional steel plate, slender b/t_s limits are given considering a non-dimensional slenderness limit of 0.7 (Report 2020; Seif and Schafer 2010), where $F_{cr} = 2f_y$. In this study, a similar approach is considered for the plate buckling on an elastic medium (i.e., concrete layer). The elastic buckling stress (σ_{cr}) in Eq. 10 is taken as $2f_y$, and the t_c/t_s ratio is calculated for various b/t_s values. The values are found for f_y = 250 MPa, 350 MPa and 450 MPa. Concrete grades considered are 30 MPa, 50 MPa and 70 MPa. The elastic modulus of steel is taken as 200 GPa, and the secant elastic modulus (E_c) in AISC-360 is considered for concrete, along with the C_3 reduction factor. The reduction in the elastic modulus is considered to account for the stiffness reduction in the concrete layer due to cracking at the point of buckling. The b/t_s versus t_c/t_s graphs plotted for f_y of 250 MPa for three different concrete grades (30 MPa, 50 MPa and 70 MPa) are shown in Fig. 3. Similarly, graphs plotted for f_y of 350 MPa and 450 MPa are shown in Figs. 4 and 5, respectively.

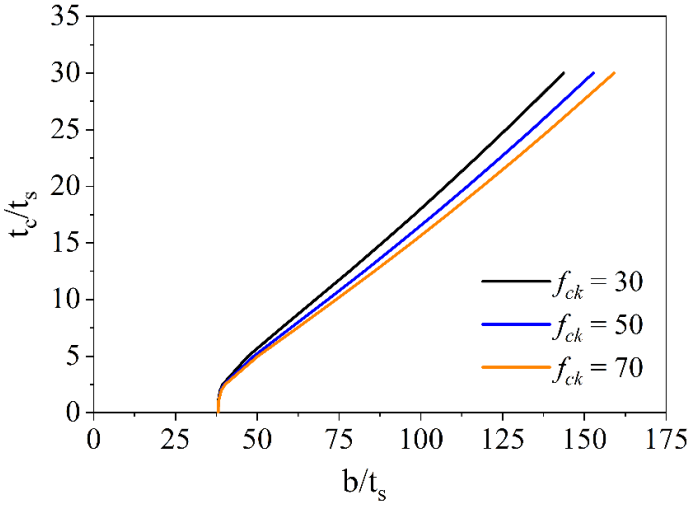

Figure 3: b/t_s versus t_c/t_s plot for f_y = 250 MPa

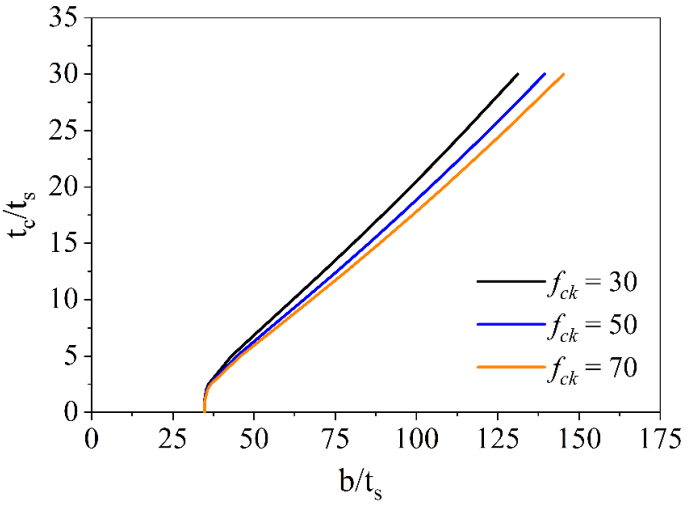

Figure 4: b/t_s versus t_c/t_s plot for f_y = 250 MPa

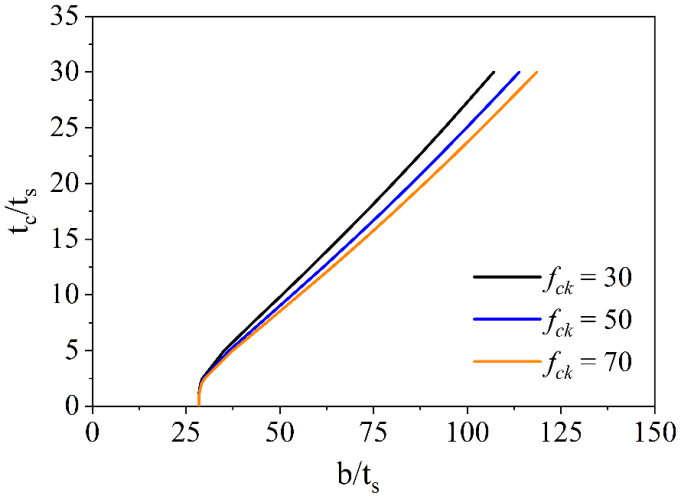

Figure 5: b/t_s versus t_c/t_s plot for f_y = 250 MPa

From the Figs. 3 – 5, it could be observed that there is no need for a concrete layer to prevent buckling when the b/t_s values are upto 39, 33 and 29, respectively, and when the steel grades are 250 MPa, 350 MPa and 450 MPa. If the values are higher than that, the requirements of t_c increase linearly. These graphs have been plotted from Eq. 10, where t_c/t_s is found iteratively for different b/t_s values using the *goal seek option* in Excel as t_c/t_s in Eq. 10 is coupled with other variables. A regression analysis is carried out using the plots in Figs. 3 – 5 to find a simple expression for t_c/t_s that will be useful for design applications. A semi-empirical formula is found in Eq. 14. The proposed expression is valid only if the b/t_s is greater than the limiting value of $1.4\sqrt{(E_s/f_y)}$. The expression in Eq. 14 is shown graphically in Fig. 6 for various steel and concrete grades.

$$\frac{t_c}{t_s} = \left[\frac{180\,f_y}{E_s} - 0.001\,f_c^{'}\right]\frac{b}{t_s} + 0.026\,f_c^{'} - 9.3 \tag{14}$$

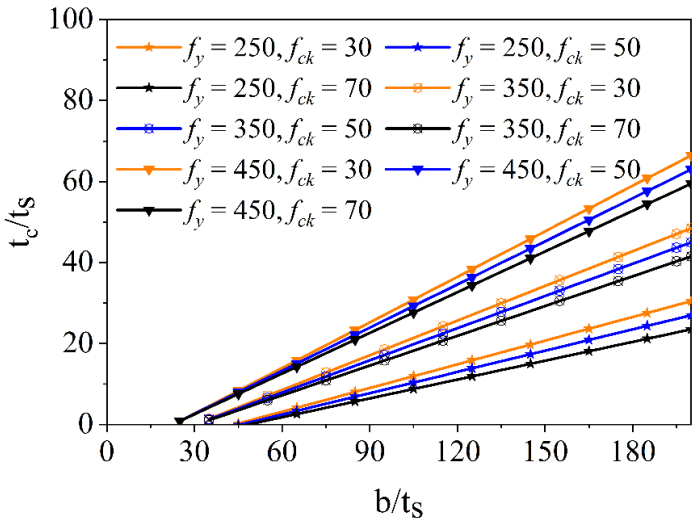

Figure 6: Graphical representation of the proposed expression

4. Comparison with experiments and code specifications

The plate buckling of a square steel tubular column can be prevented by filling the tube optimally. The minimum thickness of the concrete layer to be filled is determined using Eq. 14 for a given b/t_s value and the steel strength and concrete grade of the H-CFST column. However, this proposed expression has to be validated through experimental results. The axial compression tests done on square H-CFST specimens are collected from Praveena (2012) and Satoshi et al. (1996a). Very few researchers have worked on H-CFST, as discussed in the introduction section, and only two researchers have reported on square H-CFST. The thickness of the concrete layer (t_c) provided in the tests and the minimum concrete thickness from the proposed expression ($t_{c,\,\min}$) are compared in Table 1. The b/t_s values of the test specimens are within the limiting b/t_s value of $1.4\sqrt{(E_s/f_y)}$, and therefore, the $t_{c,\,min}$ is very low. However, the thickness provided in the tests is much larger as the objective of the tests is not to optimize the concrete layer but to evaluate the axial compressive strength equations for the H-CFST cross-section and quantify the concrete confinement. Table 1 enumerates the specimen details, where S. No. 1 – 3 are taken from Praveena (2012), and 4 – 17 are taken from Satoshi et al. (1996a). The test capacities are compared with the axial compressive

strength specified in AISC-360 for compact concrete-filled steel tubular columns (CFST). The code predictions are conservative for most of the specimens irrespective of the width-to-thickness ratio of the steel tube (b/t_s), steel yield strength (f_y) and concrete grade (f_c'). The conservativeness in the prediction decreases with the increase in the hollowness ratio for all types of width-to-thickness ratio of the steel tube (b/t_s), steel yield strength (f_y) and concrete grade (f_c'). However, it should be noted that the confinement effect is observed in H-CFST even for hollowness ratios of 50% without an inner steel tube.

Table 1: H-CFST axial compression test details from the literature

S. No.	Specimens	b (mm)	b_i (mm)	t_s (mm)	t_c (mm)	b/t_s	L/b	$t_{c,\,min}$ (mm)	f_y (MPa)	$f_{c'}$ (MPa)	P_{test} (kN)	P_{AISC} (kN)	P_{AISC}/P_{test}
1	HSS-SS-6	180	60	5	55	36	6	10	357.9	31.04	1978	1886	0.95
2	HSS-SS-12	180	60	5	55	36	12	10	357.9	31.04	1921	1786	0.93
3	HSS-SS-20	180	60	5	55	36.0	20	10	357.9	31.04	1539	1570	1.02
4	BR17H00	151	0	8.51	67	17.7	3	1	542	88.1	4572	3943	0.86
5	BR17H05	151	40	8.51	47	17.7	3	1	542	86.2	4224	3799	0.90
6	BR17H10	151	55	8.51	40	17.7	3	1	542	86.8	4164	3706	0.89
7	BR17H20	151	69	8.51	32	17.7	3	1	542	94	3899	3655	0.94
8	BR17H30	151	84	8.51	25	17.7	3	0	542	76.4	3560	3313	0.93
9	BR17H50	151	102	8.51	16	17.7	3	0	542	68.5	3151	3043	0.97
10	BR33H00	151	0	4.44	71	34.0	3	4	353	80	2753	2278	0.83
11	BR33H05	151	32	4.44	55	34.0	3	4	353	80.6	2642	2218	0.84
12	BR33H10	151	44	4.44	49	34.0	3	4	353	87.4	2606	2262	0.87
13	BR33H20	151	68	4.44	37	34.0	3	4	353	76.5	2227	1921	0.86
14	BR33H30	151	83	4.44	30	34.0	3	4	353	78.8	2089	1800	0.86
15	BR33H50	151	106	4.44	18	34.0	3	4	353	71.3	1628	1452	0.89
16	BR17M10	151	51	8.51	41	17.7	3	0	542	49.2	3720	3249	0.87
17	BR17M20	151	69	8.51	33	17.7	3	0	542	53.5	3504	3209	0.92
										Mean			0.90
										Standard deviation			0.05
										Coeff. of variation			0.06

5. Numerical Studies

The test data available from the literature is not sufficient to check the validity of the proposed expression. Therefore, numerical studies are conducted to generate more data. The hollow concrete-filled steel tubular (H-CFST) column under axial loading is simulated using the finite element software ABAQUS. The steel tube and concrete filling are modelled as two different parts. The steel tube is modelled using S4R shell elements, while the concrete core with C3D8R solid elements. Surface-to-surface interaction is defined between the steel and concrete, incorporating hard contact and with a penalty friction coefficient of 0.25. The material properties for concrete are adopted from Kent and Park (1971), considering an unconfined concrete compressive behavior combined with the CDP model to account for multiaxial stresses in concrete. The properties of steel are taken from (Byfield et al. 2005). Boundary conditions are applied using multi-point constraint (MPC) to create pinned supports at both ends of the column, and a displacement-based load is applied at one end of the column. Buckling analysis is performed prior to the axial compression simulation to account for the initial imperfections in the H-CFST specimen. The local and global buckling mode shapes from the elastic buckling analysis results are incorporated into

the model. The scale factor considered for local imperfections is 0.1*t* (Schafer et al. 2010) and *L*/1000 for global imperfections. After conducting a mesh convergence study, an element of size 10 mm is considered (*B*/18), which is in line with the suggestion in the literature (Tao et al. 2013). The model is analyzed using the static general solver.

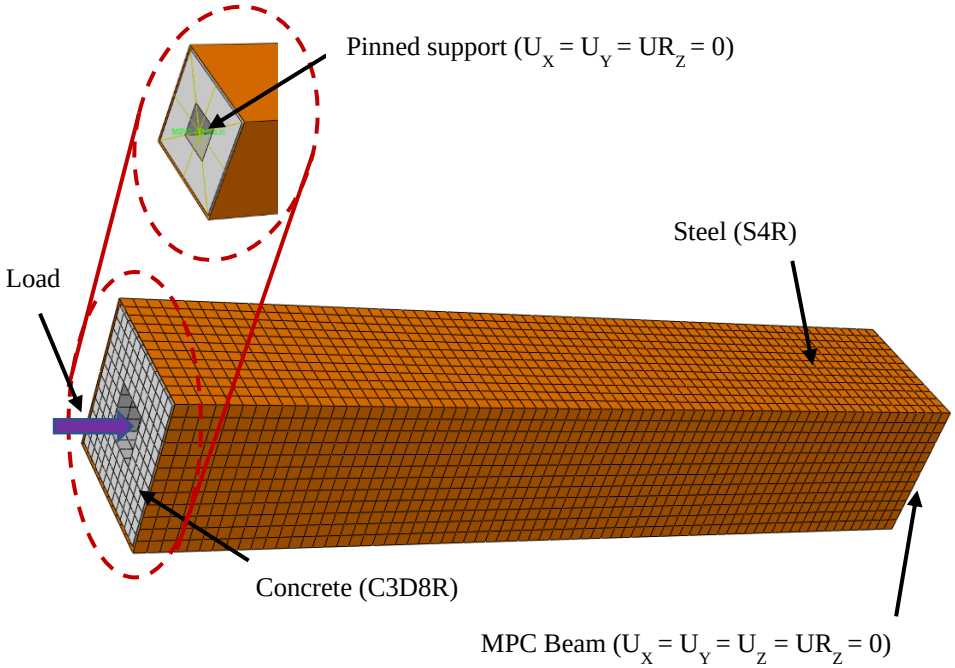

Figure 7: FE model loading and boundary condition details

5.1 Model Validation

The numerical model is validated by comparing the axial load versus deflection and strain curves with experimental results from the literature Praveena (2012). In comparison, the numerical model exhibited similar behavior in terms of initial stiffness and ultimate load (Fig. 8). This validation demonstrates the reliability of the numerical model for predicting the behavior of Hollow concrete-filled steel tubular (H-CFST) columns. The failure modes are also compared in Fig. 9, where the column has yielded first before undergoing local or global buckling.

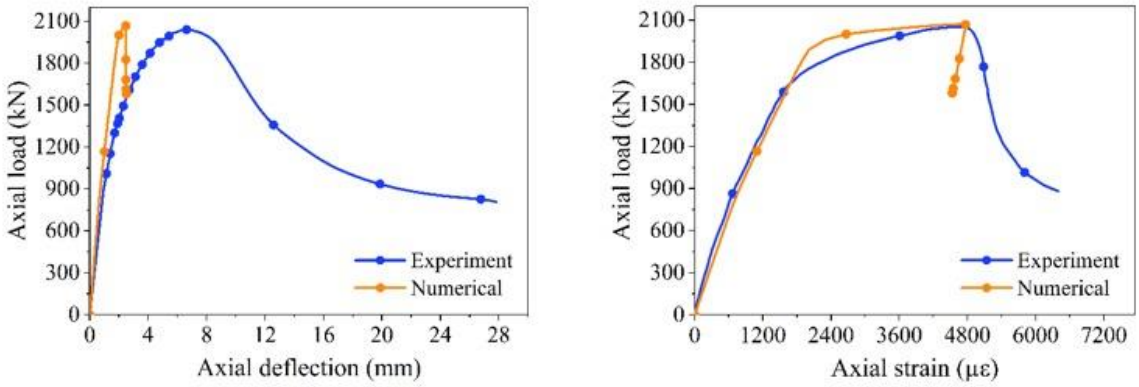

Figure 8: Validation of the FE model

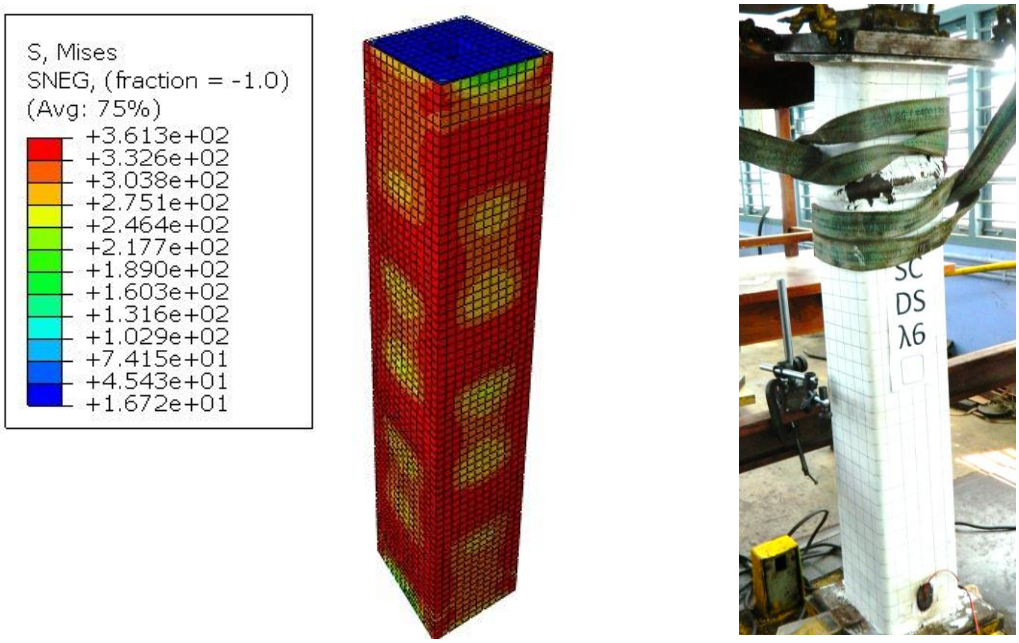

Figure 9: Failure mode comparison between the FE model and test results (Praveena, 2012)

5.2 Parametric studies

The main objective of the numerical study is to generate more data to evaluate the proposed expression. Therefore, a parametric study is conducted, varying the design parameters like the width-to-thickness ratio of the steel tube (b/t_s), steel yield strength (f_y), concrete grade (f_c'), and the length-to-width ratio (L/b). In every H-CFST model (S1 to S33), the concrete layer thickness is found from the proposed expression for the minimum concrete thickness (Eq. 14). Totally, 33 specimens are modelled and analyzed. The width-to-thickness ratio of the steel tube (b/t_s) is varied from 60 to 180, three types of steel grade are chosen (250 MPa, 350 MPa and 450 MPa), three types of concrete grades are selected (30 MPa, 50 MPa and 70 MPa), and two types of length-to-width ratio (L/b) are chosen (3 and 20). The non-dimensional member slenderness ranges from 0.08 to 0.8 for the selected column specimens. The ultimate axial compressive capacity from the post-buckling FE results is tabulated in Table 2, along with other details of the column specimens. The FE capacity is compared with the predictions using AISC-360 code specifications for a compact CFST column. It could be observed that the AISC-360 predictions are in good agreement with the FE results for most of the specimens, which suggests that the proposed concrete thickness is sufficient to prevent the local buckling in the H-CFST. However, for b/t_s of 180, the predictions are unconservative, indicating a local buckling in the steel tube before yielding. The mean and standard deviation of the code prediction to FE results are 1.03 and 0.07, respectively. The failure mode in specimen S20 and a corresponding CFST specimen is shown in Fig. 10. The failure pattern and the yield locations are comparable, which proves that the H-CFST is an improvement to CFST columns. The predictions are more conservative in the case of long columns. It should be noted that the proposed expression is derived with an assumption that the buckling plate is very long compared to the width (i.e., $L > 10b$). Further, the weight reduction in specimen S31 is 15% compared to its corresponding CFST specimen, whereas the strength reduction is only 5%. Therefore, H-CFST is a good alternative to CFST in long columns with a good strength-to-weight ratio. The results from this study will be helpful for further research in the local buckling aspects

of CFST and HCFST columns. However, experiments need to be conducted to evaluate the proposed expressions.

Table 2: Details of the specimens selected for parametric studies and capacity comparison

S. No.	Specimens	b (mm)	b_i (mm)	t_s (mm)	t_c (mm)	b/t_s	L/b	f_y (MPa)	$f_{c'}$ (MPa)	P_{FE} (kN)	P_{AISC} (kN)	P_{AISC}/P_{FE}
1	S1	180	155	3	10	60	3	250	30	708	747	1.06
2	S2	180	159	3	8	60	3	250	50	807	843	1.04
3	S3	180	163	3	5	60	3	250	70	910	897	0.99
4	S4	180	140	2	18	90	3	250	30	627	668	1.06
5	S5	180	145	2	16	90	3	250	50	783	823	1.05
6	S6	180	150	2	13	90	3	250	70	832	931	**1.12**
7	S7	180	125	1	27	180	3	250	30	516	543	**1.05**
8	S8	180	131	1	24	180	3	250	50	634	730	**1.15**
9	S9	180	137	1	20	180	3	250	70	762	870	**1.14**
10	S10	180	123	3	26	60	3	350	30	1114	1121	1.01
11	S11	180	127	3	24	60	3	350	50	1260	1336	1.06
12	S12	180	131	3	22	60	3	350	70	1609	1518	0.94
13	S13	180	107	2	34	90	3	350	30	908	952	1.05
14	S14	180	113	2	32	90	3	350	50	1056	1215	**1.15**
15	S15	180	118	2	29	90	3	350	70	1283	1443	**1.12**
16	S16	180	92	1	43	180	3	350	30	751	746	0.99
17	S17	180	99	1	40	180	3	350	50	933	1036	1.11
18	S18	180	105	1	37	180	3	350	70	1282	1290	1.01
19	S19	180	90	3	42	60	3	450	30	1562	1451	0.93
20	S20	180	94	3	40	60	3	450	50	1892	1757	0.93
21	S21	180	98	3	38	60	3	450	70	2281	2038	0.89
22	S22	180	75	2	50	90	3	450	30	1187	1193	1.01
23	S23	180	80	2	48	90	3	450	50	1494	1536	1.03
24	S24	180	85	2	45	90	3	450	70	1854	1853	1.00
25	S25	180	60	1	59	180	3	450	30	872	907	1.04
26	S26	180	66	1	56	180	3	450	50	1158	1271	**1.10**
27	S27	180	72	1	53	180	3	450	70	1483	1611	**1.09**
28	S28	180	123	3	26	60	20	350	30	920	892	0.97
29	S29	180	127	3	24	60	20	350	50	1059	1027	0.97
30	S30	180	131	3	22	60	20	350	70	1181	1138	0.96
31	S31	180	90	3	42	60	20	450	30	1266	1132	0.89
32	S32	180	94	3	40	60	20	450	50	1479	1330	0.90
33	S33	180	98	3	38	60	20	450	70	1679	1506	0.90
									Mean			1.03
									Standard deviation			0.07
									Coeff. of variation			0.07

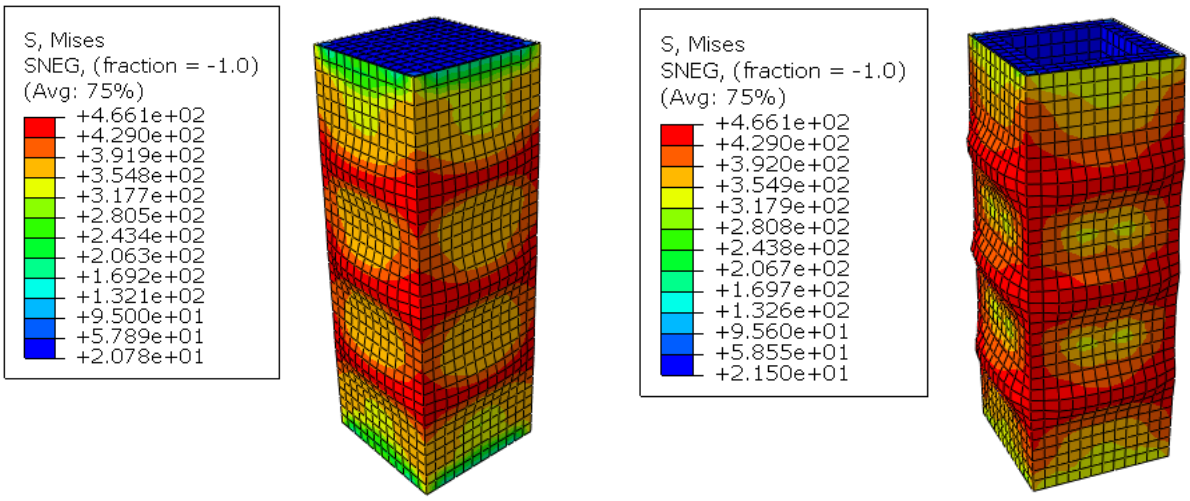

(a) CFST column (b) H-CFST column (S20)

Figure 10: Comparison of failure modes between CFST and H-CFST stub columns

6. Summary and Conclusions

Hollow concrete-filled steel tubular (H-CFST) columns have a distinct advantage over traditional CFST columns. Despite the benefits, the key challenge in the design and application is the determination of the optimal concrete wall thickness. This paper attempts to find the minimum concrete wall thickness in a square H-CFST that can delay and prevent the steel's local buckling. It is found by solving the plate buckling element supported on an elastic medium and subjected to uniform axial compression. A sinusoidal function is assumed to be the buckled shape of the plate, and the length of the plate is considered to be long, as the H-CFST's benefit over CFST is more evident in the long columns. A semi-empirical expression is proposed for determining the minimum concrete thickness based on the analytical results for design convenience. The proposed expression is validated with the test results on square H-CFST columns found in the literature. Numerical studies are carried out as the tests on square H-CFST are scarce. A finite element model is developed using ABAQUS software and validated using the test results. The following conclusions are made from the present study.

1) Optimal concrete filling of the steel tube, as in the case of H-CFST, is recommended if the objective is to prevent the local buckling of the steel tube. This concept is more useful in the case of a long CFST column, where the concrete confinement effect is lesser.
2) The minimum concrete thickness to prevent local buckling increases with the increasing width-to-thickness ratio of the steel tube and steel yield strength. It reduces with the increase in the concrete grade.
3) By optimal concrete filling, the added weight in the column is much less, with negligible reduction in the load-bearing capacity of the column for long columns.
4) Parametric studies on square H-CFST using the numerical models show that the minimum concrete thickness from the proposed expression could prevent the local buckling in the H-CFST columns. The buckling behavior is similar to that of a filled concrete steel tube (i.e., CFST). It is more satisfactory in the case of long columns.
5) The axial compression capacity of H-CFST predicted using AISC-360 is in good agreement with the FE results. The mean and standard deviation in the prediction is 1.03

and 0.07, respectively. The proposed expression predicts well for higher grade steel and for a width-to-thickness ratio lesser than 180.

6) Even though the study presents encouraging results, experiments should be conducted on short and long H-CFST columns to validate the proposed expression in determining the minimum or optimum concrete thickness.

References

1. ANSI/AISC. 2016. “Specification for Structural Steel Buildings.”
2. Byfield, M. P., J. M. Davies, and M. Dhanalakshmi. 2005. “Calculation of the strain hardening behaviour of steel structures based on mill tests.” *J. Constr. Steel Res.*, 61 (2): 133–150. https://doi.org/10.1016/j.jcsr.2004.08.001.
3. Elchalakani, M., X.-L. Zhao, and R. Grzebieta. 2002. “Tests on concrete filled double-skin (CHS outer and SHS inner) composite short columns under axial compression.” *Thin-Walled Struct.*, 40 (5): 415–441. https://doi.org/10.1016/S0263-8231(02)00009-5.
4. EN 1994-1-1. 2004. *Eurocode 4 : Design of composite steel and concrete structures Part 1-1 : General rules and rules for buildings*. *Eur. Comm. Stand.*
5. Essopjee, Y., and M. Dundu. 2015. “Performance of concrete-filled double-skin circular tubes in compression.” *Compos. Struct.*, 133: 1276–1283. https://doi.org/10.1016/j.compstruct.2015.08.033.
6. Han, L.-H., W. Li, and R. Bjorhovde. 2014. “Developments and advanced applications of concrete-filled steel tubular (CFST) structures: Members.” *J. Constr. Steel Res.*, 100: 211–228. https://doi.org/10.1016/j.jcsr.2014.04.016.
7. Han, L.-H., Z. Tao, H. Huang, and X.-L. Zhao. 2004. “Concrete-filled double skin (SHS outer and CHS inner) steel tubular beam-columns.” *Thin-Walled Struct.*, 42 (9): 1329–1355. https://doi.org/10.1016/j.tws.2004.03.017.
8. Johansson, M., and K. Gylltoft. 2002. “Mechanical Behavior of Circular Steel–Concrete Composite Stub Columns.” *J. Struct. Eng.*, 128 (8): 1073–1081. https://doi.org/10.1061/(ASCE)0733-9445(2002)128:8(1073).
9. Kuranovas, A., and A. K. Kvedaras. 2007a. “Behaviour of hollow concrete-filled steel tubular composite elements.” *J. Civ. Eng. Manag.*, 13 (2): 131–141. https://doi.org/10.1080/13923730.2007.9636429.
10. Kuranovas, A., and A. K. Kvedaras. 2007b. “Tubular Columns.” XIII (4): 297–306.
11. Kent D. C., and Park R., 1971. "Flexural Members with Confined Concrete." *Journal of Structural Division*, 97 (7): https://doi.org/10.1061/jsdeag.0002957.
12. Prasanth, M. S., and M. Sulthana. 2024a. “Experimental investigations on the partially concrete-filled steel tubular slender beams.” *Structures*, 66. Elsevier Ltd. https://doi.org/10.1016/j.istruc.2024.106862.
13. Prasanth, M. S., and M. Sulthana. 2024b. “Flexural behaviour of optimised steel tubular beams partially filled with concrete.” *Structures*, 59. Elsevier Ltd. https://doi.org/10.1016/j.istruc.2023.105749.
14. Praveena, M. 2012. “Investigations on the axial compression behaviour of composite columns.” Indian Institute of Technology Madras. (MTech Thesis)
15. Report, T. G. 2020. “Local Buckling (Width-to-thickness) Limits.” Task Group Report, AISC Committee on Specifications.
16. Romero, M. L., A. Espinos, J. M. Portolés, A. Hospitaler, and C. Ibañez. 2015. “Slender double-tube ultra-high strength concrete-filled tubular columns under ambient temperature and fire.” *Eng. Struct.*, 99: 536–545. https://doi.org/10.1016/j.engstruct.2015.05.026.
17. Satoshi M., Chiaki M., Keigo T., Tatsuo H., T. I. 1996a. “Axial compression behaviour of centrifugal concrete filled steel tubular columns using super high strength concrete.” *J. Struct. Constr. Eng. AIJ*, No. 482: 121–130.
18. Satoshi M., Chiaki M., Tatsuo H., Terutake I., Shigeru Y., K. N. 1997. “Ultimate strength and deformation capacity of centrifugal concrete filled steel tubular columns.” *J. Struct. Constr. Eng. AIJ*, No. 500: 105–112.
19. Satoshi, M., M. Chiaki, T. Keigo, H. Tatsuo, and I. Terutake. 1996b. “Evaluation formula of compressive strength of centrifugal concrete filled steel circular tubular columns using super high strength concrete.” *Jounal Struct. Constr. Eng. AIJ*, No. 482: 151–160.
20. Schafer, B. W., Z. Li, and C. D. Moen. 2010. “Computational modelling of cold-formed steel.” *Thin-Walled Struct.*, 48 (10–11): 752–762. https://doi.org/10.1016/j.tws.2010.04.008.

21. Seif, M., and B. W. Schafer. 2010. “Local buckling of structural steel shapes.” *J. Constr. Steel Res.*, 66 (10): 1232–1247. Elsevier Ltd. https://doi.org/10.1016/j.jcsr.2010.03.015.
22. Sulthana, U. M., and S. A. Jayachandran. 2017. “Axial Compression Behaviour of Long Concrete Filled Double Skinned Steel Tubular Columns.” *Structures*, 9: 157–164. Institution of Structural Engineers. https://doi.org/10.1016/j.istruc.2016.12.002.
23. Tao, Z., L.-H. Han, and X.-L. Zhao. 2004. “Behaviour of concrete-filled double skin (CHS inner and CHS outer) steel tubular stub columns and beam-columns.” *J. Constr. Steel Res.*, 60 (8): 1129–1158. https://doi.org/10.1016/j.jcsr.2003.11.008.
24. Tao, Z., Z. Bin Wang, and Q. Yu. 2013. “Finite element modelling of concrete-filled steel stub columns under axial compression.” *J. Constr. Steel Res.*, 89: 121–131. Elsevier Ltd. https://doi.org/10.1016/j.jcsr.2013.07.001.
25. Timoshenko, S. P., J. M. Gere, and W. Prager. 1962. “Theory of Elastic Stability, Second Edition.” *J. Appl. Mech.*
26. Zhao, Y. G., X. F. Yan, and S. Lin. 2019. “Compressive strength of axially loaded circular hollow centrifugal concrete-filled steel tubular short columns.” *Eng. Struct.*, 201 (October): 109828. Elsevier. https://doi.org/10.1016/j.engstruct.2019.109828.